



SEISMIC FORCE REDUCTION FACTORS FOR CONCRETE BUILDINGS REINFORCED WITH SUPERELASTIC SHAPE MEMORY ALLOY REBARS

Afrin HOSSAIN

Graduate Research Assistant, Wood Science, The University of British Columbia, Vancouver, Canada
hossain_afrin@yahoo.com

M. Shahria ALAM

Associate Professor, Ph.D., P. Eng., School of Engineering, The University of British Columbia, Okanagan, Canada
shahria.alam@ubc.ca

Ahmad RTEIL

Assistant Professor, Ph.D., P. Eng., School of Engineering, The University of British Columbia, Okanagan, Canada
ahmad.rteil@ubc.ca

ABSTRACT: In this study, the performance of newly proposed seismic-force-resisting systems, concrete reinforced with superelastic shape memory alloy (SMA) rebars, was evaluated. A trial value of the response modification coefficient, R factor was assessed and the appropriate values of system overstrength, Ω_0 and the ductility related force modification factor, R_d were determined. The FEMA P695 (2009) methodology was followed for this purpose. A total of 13 frames, varying in two parameters, building height (3 and 8) and replacement of steel by SMA starting from level 1 and moving up to the top level sequentially were analyzed. Different reinforcement detailing used for each frame were: (i) steel reinforcement in all the levels (steel-RC) and (ii) replacement of steel by SMA rebars used in the plastic hinge region of the beams in the first level and then gradually increasing the use of SMA to the upper levels and keeping steel rebar in other regions (steel-SMA-RC). For both cases, columns were reinforced with only regular steel. The frames were designed according to CSA A23.3 (2004) and assumed to be located in the high seismic zone of Western Canada. Nonlinear static pushover analyses and nonlinear incremental dynamic analyses considering 20 earthquake records were performed to investigate the seismic performance factors ($SPFs$). The obtained results on $SPFs$ of all individual frames represent that the proposed seismic factors were within the range of permissible limit and when subjected to maximum considered earthquake a sufficient margin could be provided against collapse. Steel-SMA-RC frames experienced 4%-17% lower probability of collapse compared to the steel-RC frames. This will encourage the structural and material engineers along with the builders to consider SMA as one of reinforcing materials especially in the earthquake prone areas.

1. Introduction

SMA is a unique material that has the ability of reverting to its original shape after undergoing large deformation. If SMA can be incorporated in a RC structure as reinforcing bars, then the structure will be able to dissipate seismic energy by undergoing large deformation while sustaining minimum residual deformations (Alam et al. 2008; Moni 2011; Saiidi and Wang 2006; Youssef et al. 2008). However, unlike regular steel, SMA has different mechanical properties which might change the structural response under seismic loads which requires calculating seismic performance factors ($SPFs$) for the newly proposed seismic force resisting system. Response modification, factor, R , system overstrength factor, Ω_0 and the deflection amplification factor, C_d are collectively known as the seismic performance factors ($SPFs$) (FEMA

P695 2009). Previously only a few studies have been done in this field. Alam et al. (2012) investigated the response modification factors (R_d, R_o) of RC buildings reinforced with SMA rebars where the factors were based on Canadian standards. Here, capability of a structure to dissipate energy through inelastic deformation is denoted by R_d , whereas reserve strength in a structure is denoted by R_o (NBCC, 2010). Ghassemieh and Kargarmoakhar (2013) evaluated the seismic response of steel braced frames employing SMA braces. The overall behavior of the structural systems considering the response factors was studied using static pushover analysis, *IDA* and linear dynamic analysis in terms of overstrength, ductility and response modification factors. In their study, they considered the effect of building height, number of spans, and two different types of bracings: diagonal X and Chevron on seismic performance of the structure. To date, no studies were reported that follow the more recent FEMA P695 (2009) guidelines.

The main objective of this study is to determine an appropriate value of the system overstrength factor, Ω_0 , utilizing the results from the non-linear static pushover analysis. A trial value of the response modification coefficient, R factor, and the deflection amplification factor, C_d (derived from an acceptable R value considering effective damping of the structure) will be checked afterwards utilizing the incremental non-linear dynamic analysis results to provide sufficient margin against collapse under the maximum considered earthquake for the different frames evaluated in this study.

2. Superelastic shape memory alloys

NiTi SMA microstructure has two stable phases – the high temperature and low stress phase known as austenite and the low temperature and high stress phase known as martensite. Martensite phase can be in any of two forms depending on the crystal orientation direction: twinned and detwinned. The unique properties exhibited by SMAs are the result of the transformation that occurs between these two phases (austenite and martensite) upon heating and cooling or load removal. The resulting effects associated with this phase transformation cause the material to return to its original phase due to the application of heat known as shape memory effect (SME) or after the removal of stress, known as superelasticity or pseudoelasticity (SE). Four characteristic temperatures are defined to show the transformation temperature cycle. Martensitic start temperature (M_s) at which the alloy starts to transform from austenitic to martensitic phase; martensitic finish temperature (M_f) at which the alloy completely transformed into martensitic phase; austenitic start temperature (A_s) at which the reverse transformation initiates from martensitic to austenitic phase; and finally the austenitic finish temperature (A_f) at which the martensitic alloy fully turned into austenitic alloy completing the reverse phase transformation.

Superelasticity phenomenon of SMAs, occurring only above the austenitic finishing temperature, is shown in Figure 1 (a). During loading and unloading of an austenitic SMA, six distinctive characteristics are observed in the stress-strain diagram (Figure 1 (a)); (a) the alloy is in its austenitic phase and shape when it is not subjected to any load or at low strains (<1%) (segment AB in Figure 1 (a)), (b) after the stress is induced, the alloy starts to accommodate the strain by transforming into detwinned martensitic phase at the martensitic transformation stress, σ_{MS} (segment BC in Figure 1 (a)) with a long and constant stress plateau at intermediate and large strains, (c) the alloy completely transforms into the detwinned martensitic phase when the stress reaches above σ_{MF} and the elastic response is observed at large strains (segment CD in Figure 1 (a)). Irreversible plastic deformation may occur beyond this stress level if the stress continues to increase. However, if unloaded, (d) the detwinned martensite starts to revert back to its original phase with the decreasing stress, σ_{AS} showing elastic strain recovery (segment DE in Figure 1 (a)), (e) as the stress is removed gradually, reverse transformation of unstable martensite occurs followed by a constant stress path with instinctive strain recovery (segment EF in Figure 1 (a)) (Wang et al. 2006), and (f) when the stress is very low then the alloy reverts back to its austenitic phase followed by elastic unloading (segment FA in Figure 1 (a)).

As a result, one hysteresis loop is formed during the above mentioned loading-unloading process by a closed stress-strain curve. The area formed by this loop is equal to the energy dissipation capacity of the SMA material (De Silva, 2000; Pieczyska et al., 2005) which can be also observed when SMA is subjected to cyclic axial deformation within the superelastic range. A typical stress-strain curve of austenite SMA under cyclic axial loading is shown in Figure 1 (b).

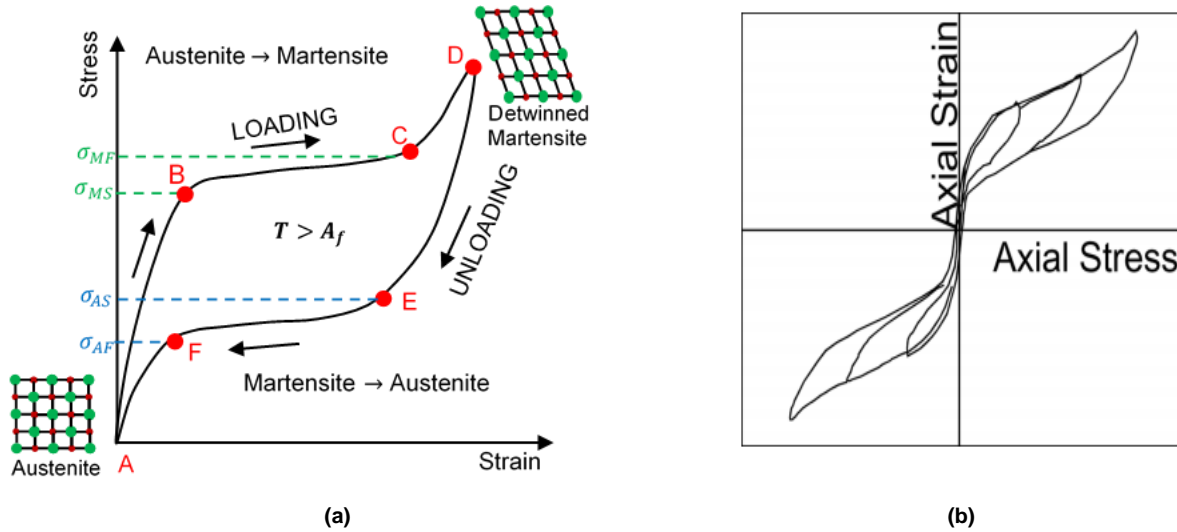


Figure 1 – (a) Superelasticity (b) Typical stress-strain diagram of superelastic SMA under cyclic axial load (Alam, Nehdi, & Youssef, 2009)

3. Overview of methodology

Seismic performance factors (*SPFs*) for different steel-SMA-RC frames were determined by iteration. The *SPFs* considered in this methodology can be defined as follows.

The Response modification coefficient, *R* factor can be defined as the ratio of the force level (V_E) that the seismic-force-resisting system would experience if it remained entirely linearly elastic under a design earthquake ground motion to the lateral force at the base of the system (i.e., base shear, V_d).

$$R = \frac{V_E}{V_d} \quad (1)$$

The system overstrength factor, Ω_0 can be defined as the ratio between the actual maximum strength of the fully-yielded system V_{max} and the design base shear, V_d .

$$\Omega_0 = \frac{V_{max}}{V_d} \quad (2)$$

The deflection amplification factor, C_d can be defined as fractional part of *R* factor.

$$C_d = \frac{\delta}{\delta_E} R \quad (3)$$

where, δ is the assumed roof drift of the yielded system corresponding to design earthquake ground motions and δ_E is the assumed roof drift of a system that remains entirely linearly elastic for design earthquake ground motion

At first, the newly proposed structural system of steel-SMA-RC frame was designed using a trial value of *R* factor which was considered the same as the value (3.5) used in steel frames (Alam et al., 2012). Non-linear structural model was developed in SeismoStruct v6 (2012). Non-linear static pushover analysis results were used to determine the system overstrength and period based ductility and non-linear *IDA* results were used to determine the median collapse spectrum to verify the initial *SPFs* values. The adequacy of the trial value of the *R* factor was validated by checking the limiting value of the adjusted collapse margin ratio (*ACMR*) (discussed in the subsequent section) suggested by FEMA P695 (2009). If the *R* factor does not satisfy the acceptable value of the adjusted collapse margin ratio, then a new trial value of *R* factor will be assumed and the whole procedure will be repeated until a satisfactory trial value of *R* factor is obtained. Then, the deflection amplification factor, C_d will be determined using the acceptable value of *R* factor. The whole process is summarized in Figure 2.

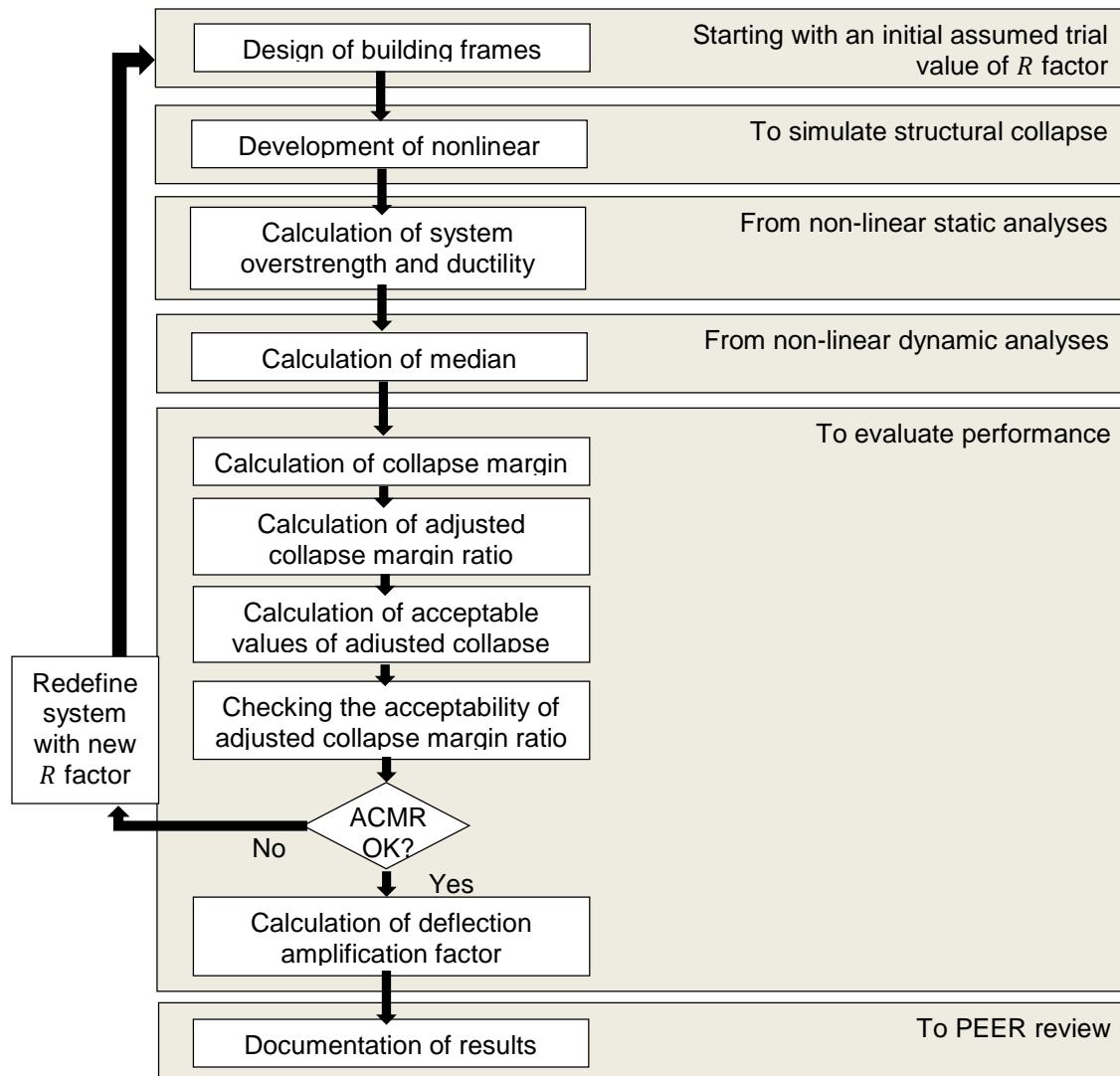


Figure 2 – Process for quantitatively establishing and documenting seismic performance factors (SPFs) (adopted from FEMA P695 (2009))

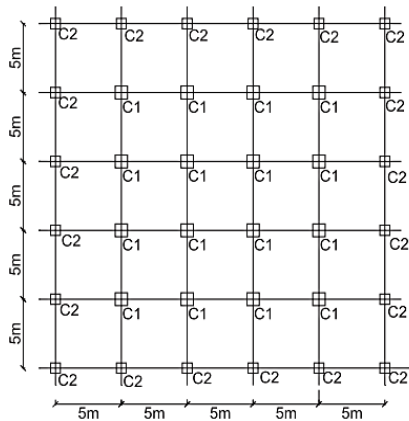
4. Buildings Design

Two different parameters have been investigated: building height (3, and 8-storeys representing low, and high rise buildings) and replacement of steel by SMA in the plastic hinge region of the beams starting from the first storey to the top storey. For this purpose, two different reinforcement detailings were used in the frames: (i) steel reinforcement along the full length of the beams at all levels (ii) replacement of steel by SMA rebars used in the plastic hinge region of the beams in the first storey only, then gradually increasing the use of SMA in the upper levels up to the top storey while steel rebars were used in other regions of the beams. Frame ID was denoted by Bh_n, where h is the building height (3 or 8) and n is the number of storeys in a frame where SMA was substitute for steel in the plastic hinge region of all the beams starting from level 1. So, for 3 and 8 storey buildings 4 and 9 frames were considered respectively which are shown in Table 1. Each frame has equidistant 5 bays of 5 m length in both directions. Three metres storey height was considered for all the frames. Two moderately ductile moment resisting steel-RC frames (B3_0 and B8_0) have been analyzed based on NBCC (2005) and designed according to CSA A23.3-04 (2004) following the equivalent static force procedure as moderately ductile moment resisting frames based on the previous work of Moni (2011). A typical plan for different building heights was similar and is shown in Figure 3 (a) and only the elevation of 3-storey frame is shown in Figure 3 (b) respectively. For different steel-SMA-

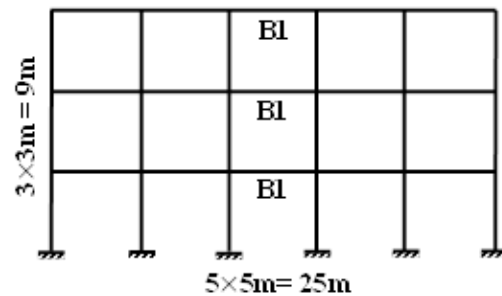
RC frames, same section sizes and reinforcement detailing (Figure 4) have been used as the steel-RC frames. The slab effect was taken into account by considering T-beam sections in the frames. Section sizes used for the beam-column members along with the reinforcement detailing according to the CSA A23.3-04 (2004) standards are tabulated in Table 2 and Table 3 respectively. The frames are assumed to be sited in Vancouver, a high seismic region in Western Canada. The material properties used for designing the frames are shown in Table 4. As SMA rebars have been applied in the plastic hinge region of the beams, the length of the plastic hinge region, L_p , had to be calculated using Paulay and Priestley (1992) equation and suggested by Alam et al. (2008) and Wang (2004) for SMA-RC elements. The rest of the beam was reinforced using steel rebars. Mechanical couplers / anchorages were assumed to be used for coupling steel and SMA rebars together (Alam et al. 2010), therefore ensuring continuous reinforcement.

Table 1 – Considered frames

Building ID	3-storey	8-storey	SMA
B3_0	B8_0	None	None
B3_1	B8_1	1 st storey only	1 st storey only
B3_2	B8_2	1 st and 2 nd storeys	1 st and 2 nd storeys
B3_3	B8_3	First 3 storeys	First 3 storeys
Frame ID		B8_4	First 4 storeys
		B8_5	First 5 storeys
		B8_6	First 6 storeys
		B8_7	First 7 storeys
		B8_8	All



(a) Plan



(b) Elevation of 3-storey

Figure 3 – Configuration of a typical 6-storey RC building (Alam et al. 2012)

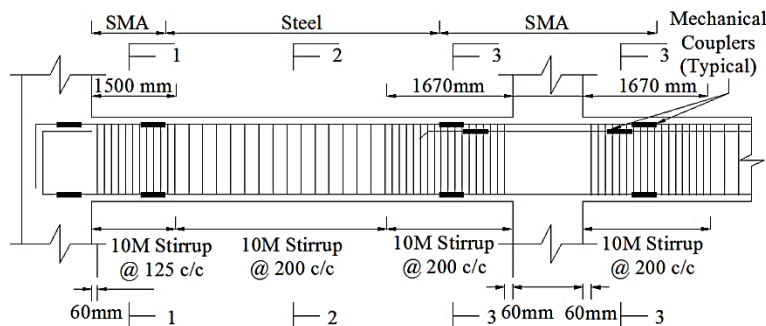


Figure 4 – Longitudinal section of beam reinforcement (Alam, Nehdi, & Youssef, 2009)

Table 2 – Column size and reinforcement arrangements

Building ID	Floor level	Column ID (Figure 2 (a))	Size (mm x mm)	Section ID Main Reinforcement (M)
3-storey	Up to roof	C1	375 x 375	8-15 M
		C2	300 x 300	4-20 M
8-storey	Up to 3 rd floor	C1	500 x 500	8-25 M
		C2	300 x 300	6-25 M
	3 rd floor to roof	C1	500 x 500	6-25 M
		C2	300 x 300	6-20 M

Table 3 – Beam reinforcement details

Building ID	Beam ID (Figure 3 (b))	Size (mm x mm)	Section ID (Figure 4)					
			Section 1-1		Section 2-2		Section 3-3	
			Main Reinforcement		Main Reinforcement		Main Reinforcement	
			Top (M)	Bottom (M)	Top (M)	Bottom (M)	Top (M)	Bottom (M)
3-Storey	B1	300 x 450	2-20	2-20	2-20	2-20	2-20	2-20
8-Storey	B1	300 x 500	3-25	4-25	3-25	4-25	5-25	4-20
	B2	300 x 500	3-20	3-20	3-20	3-20	3-20	3-20

Note: Beam B1 was used for the first three storeys, otherwise, Beam B2 was used.

Table 4 – Material properties used in the finite element analysis

Material	Mechanical property	Unit	Value
Concrete	Compressive strength	MPa	35
	Tensile strength	MPa	3.5
	Compressive strain at peak stress	%	0.2
	Compressive strain at crushing	%	0.35
Steel	Modulus of elasticity	MPa	200,000
	Yield strength	MPa	400
	Strain hardening parameter	%	0.5
SMAs	Modulus of elasticity	MPa	60,000
	Austenite to martensite starting stress	MPa	400
	Austenite to martensite finishing stress	MPa	500
	Martensite to austenite starting stress	MPa	300
	Martensite to austenite finishing stress	MPa	100
	Super elastic plateau strain length	%	6

5. Building Model

In order to perform the numerical analysis on the frames, nonlinear models of the steel-RC and steel-SMA-RC frames were developed using nonlinear finite element (FE) software SeismoStruct (2012). To account for the distribution of material nonlinearity along the length and cross-sectional area of a member, the fibre modeling approach was used. The elements used for modeling the beam-column joints were 3D beam-column inelastic displacement based frame elements. The sectional stress-strain state of those elements was obtained considering the integral nonlinear uniaxial material response of each fibre subdividing the sections according to the fibre modeling approach. All the material models used in this study were built-in in SeismoStruct (2012). For concrete, constitutive relationship of uniaxial nonlinear constant confinement model by Mander and Priestley (1988) and cyclic rules proposed by Martinez-Rueda and Elnashai (1997) were used. To present steel, uniaxial bilinear stress-strain model with kinematic strain hardening was used. SMA has been represented by the constitutive relationship of uniaxial model for superelastic shape-memory

alloy proposed by Auricchio and Sacco (1997a). Both the beams and the columns were subdivided into 4 elements longitudinally and again each element was subdivided into 200 by 200 fibre elements in the transverse direction. Two of the longitudinal elements of the beams represent the plastic hinge regions at the beam-column joint. In different steel-SMA-RC frames the beam-column joints have been modeled according to Alam et al. (2008) to take into account the SMA slippage inside the couplers (Alam et al. 2007b).

6. Nonlinear static pushover analysis

Nonlinear static pushover analysis was performed on 20 different steel-RC and steel-SMA-RC frames in order to investigate their system overstrength (Ω_0), and ductility (μ) using SeismoStruct (2012). The analysis were performed in 2D-interface. A lateral triangular load (P_0) was applied, where the vertex and the apex of the load were at the roof and base levels of the frames respectively. The applied incremental load was kept proportional in such a way ($P = P_0 \times \lambda$), where the load factor, λ , was increased monotonically by the program until a user defined limit or a numerical failure (depending on the convergence conditions at the previous step) was achieved. Response control strategy was followed in this study for the incrementation of the loading factor. It refers to direct incrementation of the global displacement (0.9 m for this study) of the top node and the calculation of the loading factor that corresponds to this target displacement.

7. Incremental Dynamic Analyses

Incremental dynamic analyses (*IDA*) (Vamvatsikos & Cornell, 2002) were performed to evaluate the nonlinear time-history response for each of the frames for a set of predefined earthquake ground motions to assess the median collapse capacities and collapse margin ratios. Each ground motion was scaled up and down to arrest a large variety of ground motion and the analyses continued until the median collapse was reached by increasing the intensities of the ground motion. Each point along the *IDA* curve was obtained performing one single nonlinear dynamic time history analysis for one frame subjected to one ground motion record scaled to one intensity level and this procedure was repeated to get the full range of *IDA* curve of response parameterized versus intensity level scaling the same ground motion record to multiple levels of intensity up to collapse. Twenty far-field (10 km or more from the fault site) earthquake ground motion records available in PEER database (PEER, 2006) were used for *IDA* to assess the frames.

8. Results

From nonlinear static pushover analyses the appropriate value of the system overstrength factor, Ω_0 was evaluated and the acceptability of the trial value of response modification coefficient, R factor was evaluated from nonlinear dynamic analyses in terms of the calculated *CMR*. Then the deflection amplification factor, C_d was evaluated from the acceptable value of R factor considering the effective damping of the seismic-force-resisting system.

8.1. Median collapse intensity and collapse margin ratio

Collapse level ground motion is defined as the median collapse when a seismic-force-resisting system experiences an intensity causing some sort of life-threatening collapse in one-half of the earthquake records considered. *CMR*, which is the primary parameter to characterize collapse assessment can be defined as the ratio between the 5%-damped median spectral acceleration of the collapse level ground motions, \hat{S}_{CT} (or corresponding displacement, SD_{CT}) and the 5%-damped spectral acceleration of the maximum considered earthquake (MCE), S_{MT} (or corresponding displacement, SD_{MT}) measured at the fundamental period of the system. MCE ground motion would cause less probability of collapse as MCE ground motions are less than the collapse level ground motions. The probability of exceedance of Vancouver hazard spectrum is 2% in 50 years (NBCC, 2010). For this reason S_{MT} was kept equal to DE spectral acceleration, S_a instead of multiplying with 1.5.

$$CMR = \frac{\hat{S}_{CT}}{S_{MT}} = \frac{SD_{CT}}{SD_{MT}} \quad (4)$$

CMR, is converted to an adjusted collapse margin ratio, *ACMR* for each building, i , in order to account for the unique characteristics of extreme ground motion (spectral shape). It was calculated using spectral shape factor, *SSF*, which depends on the system ductility (μ) and period of vibration (fundamental period, T) and is calculated from the tabulated values in FEMA P695 (2009). The system having longer period of

vibration and larger ductility is benefited by larger adjustment. Summary of collapse results are presented in Table 5.

$$ACMR_i = SSF_i \times CMR_i \quad (5)$$

Table 5 – Summary of collapse results

Frame ID	IDA results		Computed overstrength and collapse margin parameters					Acceptance Check	
	\hat{S}_{CT} (g)	S_{MT} (g)	CMR_i	μ	SPF_i	$ACMR_i$ (calculated)	β_{TOT} (assume)	$ACMR_{(code)}$	Pass /Fail
B3_0	2.24	0.820	2.73	2.67	1.16	3.17	0.5	1.90	Pass
B3_1	2.34	0.820	2.85	2.50	1.16	3.31	0.5	1.52	Pass
B3_2	2.34	0.800	2.93	2.43	1.15	3.36	0.5	1.52	Pass
B3_3	2.35	0.800	2.94	2.42	1.15	3.38	0.5	1.52	Pass
Mean of performance group			2.91	2.45	1.15	3.34	0.5	1.90	Pass
B8_0	2.56	0.404	6.34	2.38	1.20	7.60	0.5	1.90	Pass
B8_1	2.92	0.404	7.23	2.29	1.19	8.60	0.5	1.52	Pass
B8_2	2.92	0.392	7.45	2.22	1.19	8.86	0.5	1.52	Pass
B8_3	2.93	0.392	7.47	2.21	1.18	8.82	0.5	1.52	Pass
B8_4	2.93	0.379	7.73	2.21	1.18	9.12	0.5	1.52	Pass
B8_5	2.93	0.379	7.73	2.10	1.18	9.26	0.5	1.52	Pass
B8_6	3.00	0.379	7.92	2.00	1.17	9.26	0.5	1.52	Pass
B8_7	3.00	0.379	7.92	1.91	1.16	9.18	0.5	1.52	Pass
B8_8	3.00	0.379	7.92	1.88	1.16	9.18	0.5	1.52	Pass
Mean of performance group			7.67	2.10	1.18	9.05	0.5	1.90	Pass

8.2. Evaluation of collapse margin and acceptance criteria

The adjusted collapse margin ratio is compared to the acceptable criteria, which represent the collapse uncertainty. If the value is large enough, then the structure is safe with a less probability (10% for average and 20% for individual according to FEMA P695 (2009)) of collapse at MCE level ground motions and the assumed value of R factor is acceptable. If not, then a new value of R factor needs to be assumed for the next trial.

Acceptable criteria for the probability collapse of a structural system at the maximum considered earthquake, MCE ground motions is limited to 20% or less, which was set based on judgment and total system collapse uncertainty, β_{TOT} . The acceptable performance was achieved when the following two criteria were satisfied:

- Average value of calculated collapse margin ratio, \overline{ACMR}_i for the corresponding performance group exceeds $ACMR_{10\%}$:
- Collapse margin ratio for an individual frame, i with a performance group, $ACMR_i$ exceeds $ACMR_{20\%}$:

$$\overline{ACMR}_i > ACMR_{10\%} \quad (6)$$

$$ACMR_i > ACMR_{20\%} \quad (7)$$

The acceptable value of collapse margin ratio at 10% and 20% collapse probability, $ACMR_{10\%}$ and $ACMR_{20\%}$, based on $\beta_{TOT} = 0.5$ were 1.9 and 1.52 respectively from the tabulated values in FEMA P695 (2009).

From of results shown in Table 5, it can be concluded that all the values of the calculated collapse margin ratio are within the range of acceptable criteria. Not only the mean average value \overline{ACMR}_i of performance group for steel-SMA-RC frames are within the $ACMR_{10\%}$, but also each frame satisfies the criteria for both $ACMR_{10\%}$ and $ACMR_{20\%}$. This indicates that the probability of collapse for all the frames is low at MCE ground motion, especially for 8-storey buildings as the calculated value of $ACMR_i$ for all the frames are much higher than the required value mentioned in the code. Steel-SMA-RC frames experienced 4%-17%

lower probability of collapse compared to the steel-RC frames. All those results indicate that it is safe to use SMA rebars in the buildings.

8.3. Evaluation of the deflection amplification factor, C_d

The deflection modification factor, C_d is calculated from the reduced value of acceptable R factor by damping factor, B_I corresponding to system archetype damping.

$$C_d = \frac{R}{B_I} \quad (8)$$

For this study the inherent damping was assumed to be 5% of critical which gives a corresponding value of damping factor, $B_I = 1$ resulting the same value of C_d and R factor.

9. Conclusion and Future Recommendations

A total of 13 different steel-RC and steel-SMA-RC frames were analyzed based on the methodology presented in FEMA P695 (2009) using non-linear static pushover analysis and nonlinear incremental dynamic analysis. For this study, two parameters were considered: different building heights (3, 6, and 8-storeys) and gradual replacement of steel by SMA starting from level 1 to all levels in the plastic hinge region of the beams only. This gave a total of 20 different steel-RC and steel-SMA-RC frames to be considered. For all the frames the columns were reinforced with the regular steel reinforcement.

It can be concluded that all 2 steel-RC and 11 steel-SMA-RC frames of three different storeys met the FEMA P695 (2009) acceptance criteria. The proposed seismic performance factor, SPF ($R = 3.5$), was acceptable as it provided a satisfactory margin of safety against collapse when subjected to the maximum considered earthquake ground motions.

Steel-SMA-RC frames experienced 4-17% lower probability of collapse compared to the steel-RC frames. The ductility was calculated using equivalent idealized model instead of method mentioned in FEMA P695 (2009). This simplified response idealization is well representative for single degree of freedom system (SDOF) which can dissipate energy in a stable manner. Whereas for multiple degree of freedom systems (MDOF) which exhibit significant strength degradation, the definition of the effective yield displacement is more complicated and this simple equivalent bilinear model may not be very reliable in calculating ductility (Annan, Youssef, & Naggar, 2009). Damping value was assumed to be 5% of the critical value for all frames.

10. Acknowledgements

Financial contribution of Natural Sciences and Engineering Research Council of Canada (NSERC) through Discovery grant was critical to conduct this study and is gratefully acknowledged.

11. References

- Alam, M. S., Moni, M., & Tesfamariam, S. (2012). Seismic Overstrength and Ductility of Concrete Buildings Reinforced with Superelastic Shape Memory Alloy Rebar. *Engineering Structures*, 34, 8–20.
- Alam, M. S., Nehdi, M., & Youssef, M. A. (2009). Seismic Performance of Concrete Frame Structures Reinforced with Superelastic Shape Memory Alloys. *Smart Structures and Systems*, 5(5), 565–585.
- Alam, M. S., Youssef, M. A., & Nehdi, M. (2007). Seismic Behaviour of Concrete Beam-Column Joints Reinforced with Super-elastic Shape Memory Alloys. In *9th Canadian Conference on Earthquake Engineering* (p. 10). ON, Canada, Paper No. 1125.
- Alam, M. S., Youssef, M. A., & Nehdi, M. (2008). Analytical Prediction of the Seismic Behaviour of Superelastic Shape Memory Alloy Reinforced Concrete Elements. *Engineering Structures*, 30(12), 3399–3411. doi:10.1016/j.engstruct.2008.05.025
- Alam, M. S., Youssef, M. A., & Nehdi, M. (2010). Exploratory Investigation on Mechanical Anchors for Connecting SMA Bars to Steel or FRP Bars. *Materials and Structures*, 43(1), 91–107(17).
- Annan, C. D., Youssef, M. A., & Naggar, M. H. E. (2009). Seismic Overstrength in Braced Frames of Modular Steel Buildings. *Journal of Earthquake Engineering*, 13(1), 1–21. doi:10.1080/13632460802212576
- Auricchio, F., & Sacco, E. (1997). A Superelastic Shape-Memory Alloy Beam Model. *Journal of Intelligent Material Systems and Structures*, 8(6), 489–501.
- CSA A23.3. (2004). *Design of Concrete Structures, 5th ed.* Canadian Standards Association, Rexdale, ON, Canada.
- CSA A23.3-04. (2004). *Design of Concrete Structures, 5th ed.* Canadian Standards Association, Rexdale, ON, Canada.

- CSA O86. (2009). *Engineering Design in Wood*. Mississauga, Canada.
- De Silva, C. W. (2000). *Vibration: Fundamentals and Practice*. CRC Press.
- FEMA P695. (2009). *Quantification of Building Seismic Performance Factors*. Federal Emergency Management Agency, Washington, D.C.
- Ghassemieh, M., & Kargarmoakhar, R. (2013). Response Modification Factor of Steel Frames Utilizing Shape Memory Alloys. *Journal of Intelligent Material Systems and Structures, Published* . doi:10.1177/1045389X12471869
- Ibarra, L., Medina, R., & Krawinkler, H. (2002). Collapse Assessment of Deteriorating SDOF Systems. In *Proceedings, 12 th European Conference on Earthquake Engineering*. London, Elsevier Science Ltd, paper #665.
- Mander, J., & Priestley, M. (1988). Theoretical Stress–Strain Model for Confined Concrete. *ASCE J Struct Eng*, 114(8), 1804–26.
- Martinez-Rueda, J., & Elnashai, A. (1997). Confined Concrete Model under Cyclic Load. *Mater Struct*, 30, 139–47.
- Moni, M. (2011). *Performance of Shape Memory Alloy Reinforced Concrete Frames under Extreme Loads*. M.A.Sc. Thesis, Department of Civil Engineering, University of British Columbia.
- NBCC. (2005). *National Building Code of Canada, Canadian Commission on Building and Fire Codes*. Ottawa: National Research Council of Canada.
- NBCC. (2010). *National Building Code of Canada, Canadian Commission on Building and Fire Codes*. Ottawa: National Research Council of Canada.
- Paulay, T., & Priestley, M. (1992). *Seismic Design of Reinforced Concrete and Masonry Buildings*. New York: John Wiley & Sons, Inc.
- PEER. (2006). *NGA Database, Pacific Earthquake Engineering Research Center*. University of California, Berkeley, California.
- Pieczyska, E., Gadaj, S., Nowacki, W. K., Hoshio, K., Makino, Y., & Tobushi, H. (2005). Characteristics of Energy Storage and Dissipation in TiNi Shape Memory Alloy. *Sci. Technol. Adv. Mater*, 6(8), 889–894.
- Saiidi, M. S., & Wang, H. (2006). Exploratory Study of Seismic Response of Concrete Columns with Shape Memory Alloys Reinforcement. *ACI Structural Journal*, 103(3), 436–442.
- SeismoStruct. (2012). *User Manual, Version 6*. Pavia, Italy. Seismo-Soft Inc. Supporting Services.
- Vamvatsikos, D., & Cornell, C. A. (2002). Incremental Dynamic Analysis. *Earthquake Engineering & Structural Dynamics*, 31(3), 491–514. doi:10.1002/eqe.141
- Wang, H. (2004). *A Study of RC Columns with Shape Memory Alloy and Engineered Cementitious Composites*. M.Sc. Thesis, University of Nevada, Reno, Nev, USA.
- Wang, R., Cho, C., Kim, C., & Pan, Q. (2006). A proposed Phenomenological Model for Shape Memory Alloys. *Smart Mater. Struct.*, 15(2), 393–400.
- Youssef, M. A., Alam, M. S., & Nehdi, M. (2008). Experimental Investigation on the Seismic Behaviour of Beam-Column Joints Reinforced with Superelastic Shape Memory Alloys. *Earthquake Eng*, 12(7), 1205–22.